An Upgraded SGSLR Link Analysis Which Includes the Effects of Atmospheric Scintillation and Target Speckle

John J. Degnan

Sigma Space Corporation, 4600 Forbes Blvd., Lanham, MD 20706 USA

John.degnan@sigmaspace.com

1. INTRODUCTION

The link equation determines the signal strength, in photoelectrons, received from the satellite [1] and can be written in the form

$$n_s = \frac{E_t}{h\nu}\eta_t \frac{2}{\pi(\theta_d R)^2} \exp\left[-2\left(\frac{\Delta\theta_p}{\theta_d}\right)^2\right]\left[\frac{1}{1+\left(\frac{\Delta\theta_j}{\theta_d}\right)^2}\right]\left(\frac{\sigma A_r}{4\pi R^2}\right)\eta_r\eta_c T_a^2 T_c^2$$

where the hardware variables associated with SGSLR are defined and tabulated in Table 1.

VARIABLE	SYMBOL	VALUE
Laser Pulse Energy	E_t	1.5 mJ
Laser Repetition Rate	f_L	2 kHz
Transmit Optics Efficiency	η_t	0.766
Receive Optics Efficiency	η_r	0.542
Detector Counting Efficiency	η_c	0.28
Spectral Filter Efficiency	η_f	0.7
Effective Receive Aperture	A_r	0.187 m^2
Tracking Pointing Bias	$\Delta\theta_p$	2 arcsec (Sigma Range Receiver)
Telescope RMS Pointing Jitter	$\Delta\theta_J$	2 arcsec
Full Transmitter Divergence	$2\theta_d$	28 arcsec (Starlette, LAGEOS) 14 arcsec (GNSS)
Coherence Length	ρ_0	2.5 cm (Worst Case: GGAO)
Zenith Log Amplitude Variance	$C_l^s(0)$	0.054 (Worst Case: GGAO)

Table 1. Link equation parameter definitions and values for NASA's SGSLR. Most relate to the expected SGSLR hardware performance but the bottom two are atmospheric parameters reflecting the low elevation of the Goddard site.

In the following sections, we will concentrate on atmospheric effects that affect SGSLR performance. The background and derivations of most effects can be found in [1] but we add two new ones, i.e. the effects of scintillation (fading of the signal) due to atmospheric turbulence and target speckle and look at their effects on signal returns for three representative satellites – Starlette, LAGEOS, and GNSS.

2. ATMOSPHERIC EFFECTS
2.1 Atmospheric Attenuation

The atmospheric attenuation coefficient decreases approximately exponentially with altitude, h, according to the equation [1]

$$\sigma_{atm}(\lambda,V,h) = \sigma_{atm}(\lambda,V,0)\exp\left(-\frac{h}{h_v}\right)$$

where V is the sea level visibility and h_v = 1.2 km is a visibility scale height. Thus, the one way attenuation for a SLR station at elevation h_g above sea level to a satellite is

$$T_{atm}(\lambda,V,h_g) = \exp\left[-\sec\theta_{zen}\int_{h_g}^{\infty}\sigma_{atm}(\lambda,V,h)dh\right] = \exp\left[-\sigma_{atm}(\lambda,V,0)h_v\sec(\theta_{zen})\exp\left(-\frac{h_g}{h_v}\right)\right]$$
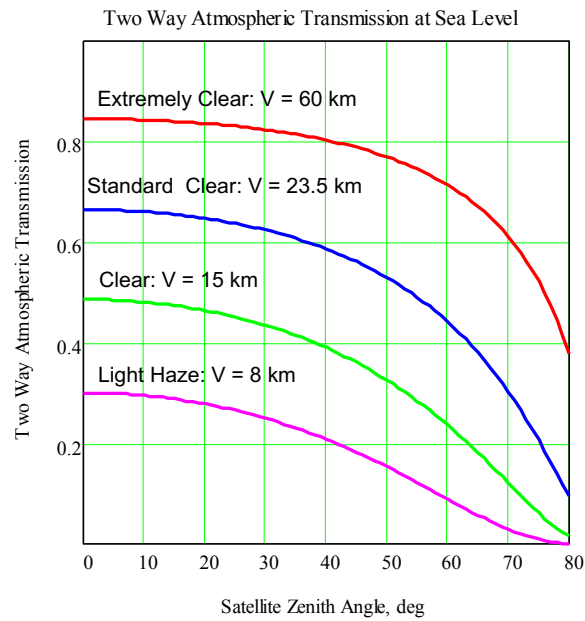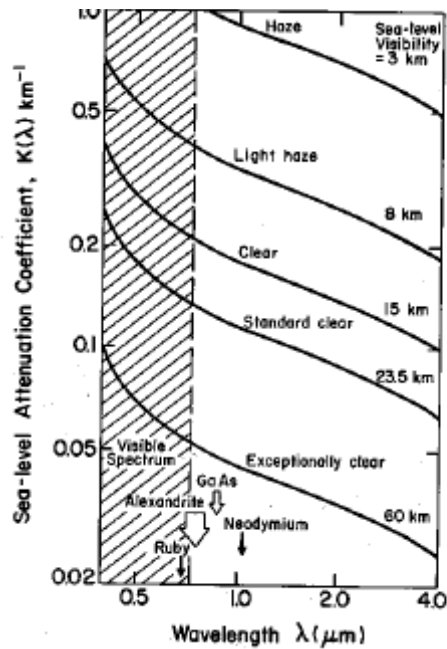

Figure 1: (a) Sea level atmospheric absorption coefficient as a function of wavelength and atmospheric visibility. (b) Two way atmospheric transmission as a function of visibility (V =60 to 8 km) and satellite zenith angle (θs = 0 to 80 deg).

2.2 Mean Cirrus Cloud Transmission

Experimentally, it is found that the one-way cirrus cloud transmission is given by

$$T_c = \exp\left[-0.14(t\sec\theta_{zen})^2\right]$$

where t is the cirrus cloud thickness. Typically, cirrus clouds are present about 50% of the time above most locations. The probability of having a certain thickness is given by the plot on the left and the computation of the mean two-way cirrus transmissions on the right. The computation of the mean includes the assumption that there are no cirrus clouds (i.e. T_c = 1) 50% of the time.
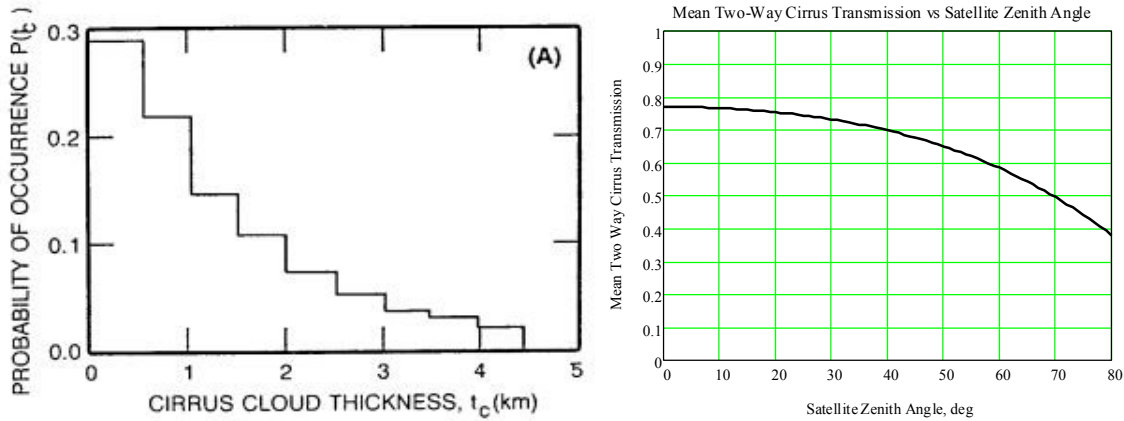
Figure 2: Left, probability of encountering a cirrus cloud with thickness, tc, in 0.5 km steps; Right, Mean Two-Way Cirrus Cloud transmission.

2.3 Atmospheric Turbulence

Atmospheric turbulence affects return signal strength in three ways [1]:

1. Beam Wander – random translations of the spatial centroid of the beam generally caused by beam passage through large turbulent eddies

2. Beam Spread – short term growth in the effective beam divergence produced by smaller eddies in the beam path

3. Scintillation or "beam fading" – responsible for the familiar "twinkling" of starlight

Effects 1 and 2 are often discussed together in terms of a "long term beam spread" defined as [1]

$$\langle \theta_L \rangle = \theta_d \sqrt{1 + \left(\frac{\omega_0}{\rho_0}\right)^2} = \frac{\lambda}{\pi \omega_0} \sqrt{1 + \left(\frac{\omega_0}{\rho_0}\right)^2} = \frac{\lambda}{\pi} \sqrt{\frac{1}{\omega_0^2} + \frac{1}{\rho_0^2}} \approx \frac{\lambda}{\pi \rho_0} \ for \ \omega_0 >> \rho_0$$

where θ_d is the transmitter beam half-divergence angle out of the telescope, ω_0 is the Gaussian beam radius at the telescope exit aperture, and ρ_0 is the "transverse atmospheric coherence length" defined by

$$\rho_0 = \left\{ 1.46 k^2 \int_{h_s}^{h_{\lim}} dh C_n^2(0) m^{-2/3} \right\}^{-3/5}$$

and $C_n^2(0)$ is the "optical strength variance" [1].

The impact of the third turbulence effect, scintillation, on the uplink causes the beam intensity to vary at the satellite retroreflectors while, on the downlink, the signals from individual retroreflectors also vary in intensity ("target speckle") but experience some "aperture averaging" at the receive telescope. Furthermore, the impact of turbulence on the uplink is much greater than on the downlink because the atmospheric phase disturbances occur far from the satellite on the uplink while, on the downlink, they occur much closer to the receive telescope. Figure 3 provides the equation used to compute the probability distribution function that one will detect n photoelectrons when, in the absence of scintillation and speckle, one would expect a mean of n_s

photoelectrons. The distributions are plotted for two satellites, Starlette and LAGEOS, and for four different satellite zenith angles, θ_z =0, 40, 60, and 80 degrees. The vertical dashed lines at y =n/n$_s$ = 1 show that, although the signal is sometimes enhanced by the scintillation (n>n$_s$), it most often is decreased (n<n$_s$), especially at larger satellite zenith angles.

$$p_T\left(n,\theta_z\right)=\frac{1}{2y(C-1)!\sqrt{2\pi C_l^s\left(\theta_z\right)}}\int_0^\infty\left(\frac{yC}{x}\right)^C\exp\left(-\frac{yC}{x}\right)\exp\left[-\frac{\left(\frac{1}{2}\ln(x)+C_l^s\left(\theta_z\right)\right)^2}{2C_l^s\left(\theta_z\right)}\right]dx$$

C = nominal number of retroreflectors aperture averaged at the receiver.
X = irradiance/mean irradiance at satellite; y = fraction of mean photoelectrons detected in the absence of scintillation
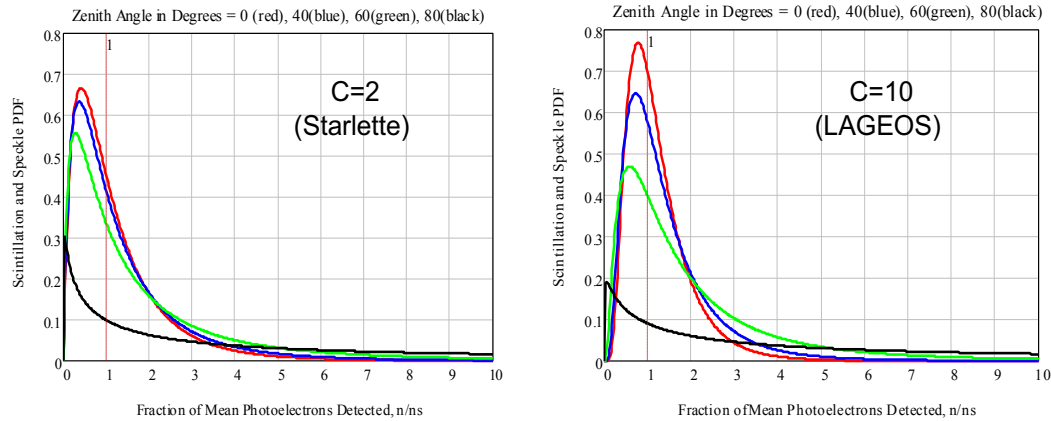

Figure 3: Combined scintillation and speckle PDF as a function of y = n/n$_s$ and four satellite zenith angles - θ_z = 0(red), 40 (blue), 60 (green) and 80 degrees (black) . (a) Starlette (C=2) ; (b) LAGEOS (C =10).

3.   SATELLITE LINK CALCULATIONS

In this Section, we compute and plot the probability of detection and the integration time required for SGSLR to generate a 1mm RMS normal point (NP) as a function of atmospheric quality (visibility V = 60 km to 8 km) and the satellite zenith angle for three representative satellites – Starlette, LAGEOS, and GNSS. In computing the probability of detection, we use the tabulated ILRS target cross-section values for Starlette and LAGEOS and the ILRS-recommended cross-section of 1×10^8 m^2 for GNSS satellites which does not necessarily apply to all GNSS satellites currently in orbit. The time required to generate a 1mm NP is given by

$$\tau_{np}=\frac{N}{P_df_L}=\frac{1}{\left(1-e^{-n_s}\right)f_L}\left(\frac{\sigma_{ss}}{\sigma_{np}}\right)^2$$

where P_d=1-exp(-n_s) is the probability of detecting a satellite return, n_s is the mean number of signal photoelectrons per pulse computed from the link equation(1), f_L = 2 kHz is the SGSLR pulse repetition rate, σ_{ss} is the single shot precision of the range measurement including both instrument and satellite contributions, and σ_{np} = 1mm is the desired NP precision. Each graph in Figure 4 contains four plots corresponding to different atmospheric conditions and visibilities, i.e. Red = Extremely Clear (V = 60 km), Blue = Standard Clear (V = 23 km) , Green = Clear (V = 15 km) ,

and Black = Light Fog (V = 8 km). Since we also assume a fixed transmitter beam divergence for the entire range of satellite zenith angles, the probability of detection in all cases falls from a maximum at zenith (θ_s = 0 deg) to fairly low values at high zenith (low elevation) angles due to both the increased range and relatively severe atmospheric losses described in earlier sections. The values used are summarized in Table 2 for the three satellites.

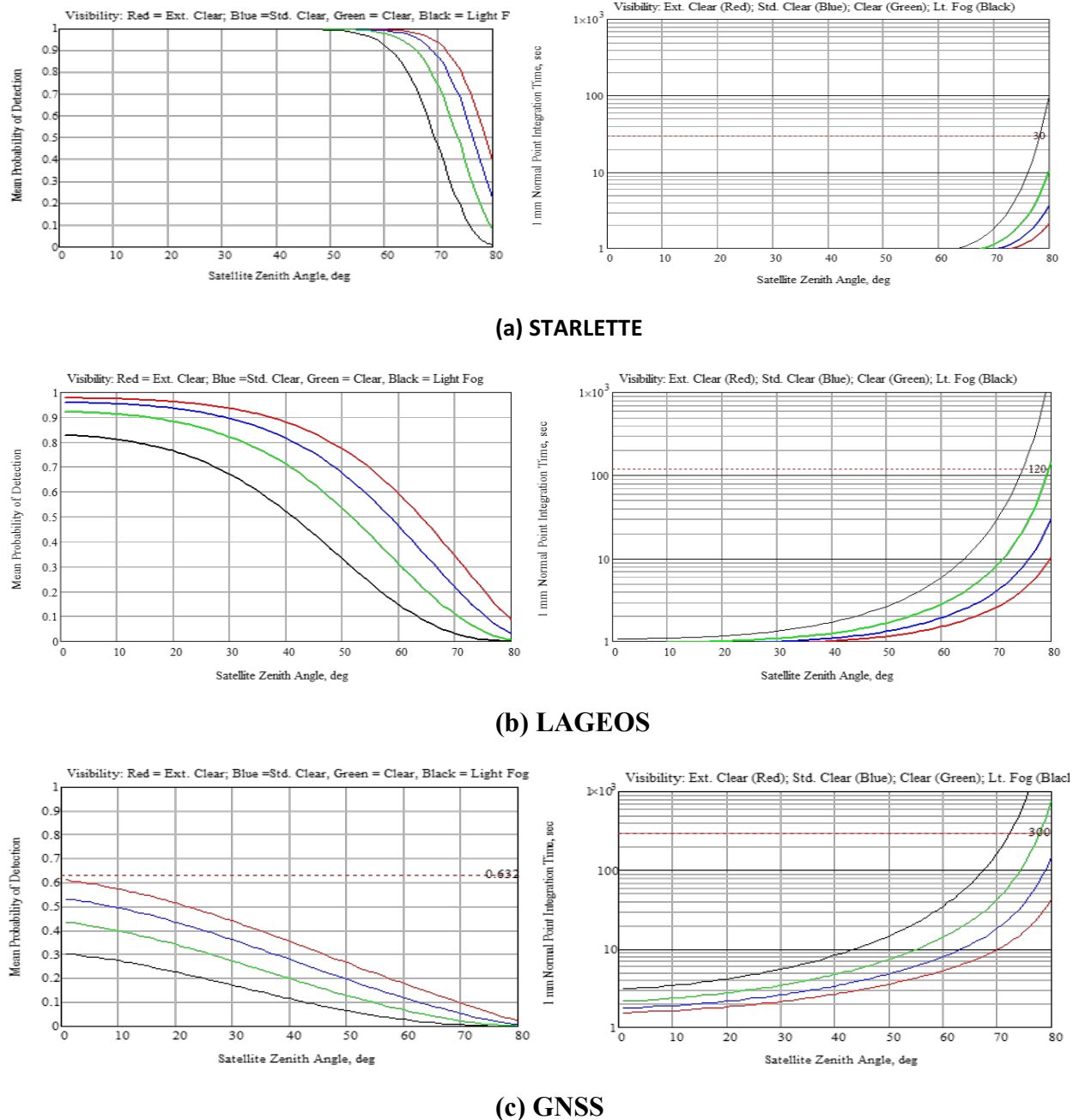**(a) STARLETTE**

(b) LAGEOS

(c) GNSS

Figure 4: Mean probability of detection and minimum time required by SGSLR to generate a 1 mm normal point for (a) STARLETTE, (b) LAGEOS, and (c) GNSS. The horizontal dashed red line in the right hand figures corresponds to the current normal point integration times recommended by the ILRS.

Satellite	Altitude (km)	Cross-section, σ (m^2)	Beam Divergence (arcsec)	Number of Retroreflectors contributing to return, C
Starlette	950	1.8×10^6	28	2
LAGEOS	6,000	15×10^6	28	10
GNSS	20,000	100×10^8	14	48

Table2: Characteristics of representative satellites used in this analysis.

4. SUMMARY

The SGSLR link analyses presented considered the following effects:
1. SLR System
   - laser energy (1.5 mJ) and fixed beam divergence (14 arcsec for GNSS or 28 arcsec for Starlette and LAGEOS)
   - detector PDE (~28%)
   - transmit (77%) and receive (54%) optical throughput efficiencies, spectral filter (70%) and obscurations (secondary mirror and transmit injection mirror)
   - telescope pointing bias and jitter (2 arcsec each during tracking with automated pointing correction provided by SGSLR multifunctional receiver [2])
2. Target
   - Optical cross-section (from ILRS tables/recommendations)
   - Target speckle effects
3. Atmosphere
   - Atmospheric transmission vs ground visibility - extremely clear (60 km), standard clear (23 km), clear (15 km) and light fog (8 km)
   - Mean cirrus cloud transmission
   - Worst case atmospheric turbulence effects (GGAO): short and long term beam wander, uplink scintillation (downlink is negligible)
   - Telescope aperture averaging of target speckle effects.

The wide variation in signal strength as a function of satellite zenith angle suggests having the ability to reduce the beam divergence at low elevation angles in order to increase the data rate and reduce the normal point integration time.

REFERENCES

[1] J. Degnan, Millimeter Accuracy Satellite Laser Ranging: A Review, in Contributions of Space Geodesy to Geodynamics: Technology, D. E. Smith and D. L. Turcotte (Eds.), AGU Geodynamics Series, Volume 25, pp. 133-162, 1993.

[2] J. Degnan, R. Machan, E. Leventhal, D. Reed, J. Marzouk, Progress on the Multifunctional Range Receiver for SGSLR, 20th International Workshop on Laser Ranging, Potsdam, Germany, October, 2016.